Physica B 405 (2010) 2930–2934

Contents lists available at ScienceDirect

Physica B

journal homepage: www.elsevier.com/locate/physb

Current-driven metamaterial homogenization

Chris Fietz *, Gennady Shvets

University of Texas at Austin, Department of Physics, Austin, TX 78712, USA

ARTICLE INFO

Keywords:
Metamaterial homogenization
Constitutive parameters
Metamaterial antenna

ABSTRACT

A current-driven homogenization (CDH) approach to calculating all 36 linear constitutive parameters of a metamaterial crystal is presented. Spatial dispersion is accounted for by evaluating the constitutive parameters as a function of frequency and wavenumber. For two-dimensional centrosymmetric crystals spatial dispersion is shown to result in bianisotropy. The accuracy of the CDH constitutive parameters is verified by comparing the radiation efficiencies of a simple directional antenna embedded inside the homogenized and un-homogenized metamaterial slabs.

1. Introduction

Since the invention of artificial materials with negative magnetic response about a decade ago [1], considerable work has gone into the study of electromagnetic metamaterials (artificial materials engineered to have exotic optical properties). In that time both analytic [1,2] and numerical [3–6] methods have been suggested for determining the constitutive parameters of such metamaterials. Although analytic expressions are useful for approximating a metamaterial's response and providing general intuition, ultimately numerical methods are needed to accurately calculate constitutive parameters. The full constitutive parameters matrix (CPM), which relates the electric and magnetic induction vectors **D** and **B** to the electric and magnetic fields **E** and **H** according to Eq. (1), has 36 components. Currently, all proposed numerical methods are severely limited to extracting a small number of the total 36 entries of the CPM. In this paper we outline a numerical procedure, current-driven homogenization (CDH), for calculating all components of the CPM as a function of ω and $\mathbf{k}$.

An important aspect of the CDH method is that it enables computing constitutive parameters for frequencies and wavenumbers both on and off of the dispersion curve $\omega=\omega(\mathbf{k})$. Up to now, research has only focused on the behavior of metamaterials on the dispersion curve. However, applications such as, for example, novel antennas embedded in metamaterial shells, require the calculation of constitutive parameters both on and off the dispersion curve, i.e. for arbitrary and unrelated ω and $\mathbf{k}$. To the best of the authors' knowledge, the CDH is the first approach to calculating the constitutive parameters of a metamaterial crystal away from the dispersion curve.

Essential to the CDH approach is the idea of driving a metamaterial crystal with both electric and magnetic charge-current. In Section 2 we explain why this is necessary and how it enables us to extract all 36 parameters of the CPM. In addition to driving the crystal, a field averaging procedure which converts the microscopic EM fields in a metamaterial into averaged (macroscopic) EM fields is required. The method of driving the crystal with electric and magnetic charge-current is independent of the averaging procedure used and different field averaging procedures can be used interchangeably. In Section 3, a new field averaging procedure is described that is particularly accurate at providing approximately correct boundary conditions. Finally, in Section 5 we calculate the constitutive parameters for a two-dimensional plasmonic crystal and then validate the extracted parameters by calculating the transmission of a simple metamaterial antenna driven with a wide spectrum of **k**'s.

2. Current driven extraction of the constitutive parameters

First, we consider the procedure of extracting the constitutive parameters of a homogeneous medium. The most common definition of the constitutive parameters matrix (CPM) is

$$\begin{pmatrix}\mathbf{D}\\ \mathbf{B}\end{pmatrix}=\begin{pmatrix}\varepsilon & \xi\\ \zeta & \mu\end{pmatrix}\begin{pmatrix}\mathbf{E}\\ \mathbf{H}\end{pmatrix}, \tag{1}$$

where the field vectors **D**, **B**, **E** and **H**, are the macroscopic electromagnetic induction and field vectors, respectively. The 6×6 CPM is, by convention, separated into four 3×3 matrices known as ε, ξ, ζ and μ [7]. Because the most general CPM contains 36 unknown entries, we need 36 linearly independent equations of constraint to calculate it. A single set of EM fields related through Eq. (1) provides six equations of constraint. Therefore we need six sets of linearly independent EM fields obeying Eq. (1) to compute the

* Corresponding author.
E-mail address: cfietz@physics.utexas.edu (C. Fietz).

0921-4526/$ - see front matter © 2010 Elsevier B.V. All rights reserved.
doi:10.1016/j.physb.2010.01.006

CPM. Specifically, we need six linearly independent sets of field vectors providing us with 36 equations of constraint that can be solved for 36 unknowns. Of course, the CPM of a homogeneous medium is known, so what is described in this section is merely an extraction procedure that recovers the *a priori* known CPM.

If we use only EM waves supported by the medium free of source terms (either propagating or evanescent waves), as it is conventionally done in the context of metamaterials [3,4], then for a general material only one set of linearly independent fields is available for a particular set of $[\omega, \mathbf{k}(\omega)]$, where $\omega = \omega(\mathbf{k})$ is the dispersion relation. Three sets of linearly independent fields can be obtained by driving the metamaterial crystal with electric charge-current [6], but six sets are needed. A solution to our problem becomes apparent when we inspect a modified form [8,9] of the Maxwell equations in a *homogeneous* medium:

$$\nabla \cdot \mathbf{D} = 4\pi\rho, \quad \nabla \times \mathbf{H} - \frac{1}{c}\frac{\partial \mathbf{D}}{\partial t} = \frac{4\pi}{c}\mathbf{J},$$

$$\nabla \cdot \mathbf{B} = 4\pi\phi, \quad -\nabla \times \mathbf{E} - \frac{1}{c}\frac{\partial \mathbf{B}}{\partial t} = \frac{4\pi}{c}\mathbf{I}, \tag{2}$$

where the magnetic charge density ϕ and magnetic current density $\mathbf{I}$ are introduced. In a homogeneous medium an electric current $\mathbf{J} = \mathbf{J}_0 e^{i(\omega t - \mathbf{k}\cdot\mathbf{x})}$ and magnetic current $\mathbf{I} = \mathbf{I}_0 e^{i(\omega t - \mathbf{k}\cdot\mathbf{x})}$ that are harmonic in time and space will generate an EM wave $\mathbf{E}(t,\mathbf{x}) = \mathbf{E}_0 e^{i(\omega t - \mathbf{k}\cdot\mathbf{x})}$ and $\mathbf{H}(t,\mathbf{x}) = \mathbf{H}_0 e^{i(\omega t - \mathbf{k}\cdot\mathbf{x})}$ according to Eq. (2), which can be rearranged in ω and $\mathbf{k}$ space and combined with the constitutive matrices yielding

$$\mathcal{M}\begin{pmatrix}\mathbf{E}_0\\ \mathbf{H}_0\end{pmatrix} = \frac{4\pi i}{c}\begin{pmatrix}\varepsilon^{-1}\mathbf{J}_0\\ \mu^{-1}\mathbf{I}_0\end{pmatrix}, \tag{3}$$

where

$$\mathcal{M} = \begin{pmatrix}\omega/c & \varepsilon^{-1}(\mathbf{k}\times + \omega\xi/c)\\ -\mu^{-1}(\mathbf{k}\times - \omega\zeta/c) & \omega/c\end{pmatrix}. \tag{4}$$

Here the four blocks of the $\mathcal{M}$ matrix are represented by 3×3 matrices, and $(\mathbf{k}\times)_{ij} \equiv \varepsilon_{ijl}k_l$. All four constitutive matrices are assumed to be functions of ω and $\mathbf{k}$. If ω and $\mathbf{k}$ do not lie on the dispersion curve of the metamaterial crystal (i.e. do not satisfy the $\omega = \omega(\mathbf{k})$ dispersion relation), then $\mathcal{M}$ is invertible and $\mathbf{E}_0$ and $\mathbf{H}_0$ can be solved for. Therefore, if we limit ourselves to electric current only, then at most three linearly independent field vectors are obtained. Those would be insufficient for solving Eq. (1) for the constitutive parameters. However, if we allow ourselves to drive the metamaterial crystal with both electric and magnetic current, then six linearly independent field vectors can be obtained. These can be used for extracting all entries of the CPM from Eq. (1). Explicitly, the extraction procedure is as follows. First, the following 6×6 EM field matrices are defined:

$$\mathcal{D} \equiv \begin{pmatrix}\mathbf{D}_0^1, \mathbf{D}_0^2, \ldots, \mathbf{D}_0^6\\ \mathbf{B}_0^1, \mathbf{B}_0^2, \ldots, \mathbf{B}_0^6\end{pmatrix},$$

$$\mathcal{E} \equiv \begin{pmatrix}\mathbf{E}_0^1, \mathbf{E}_0^2, \ldots, \mathbf{E}_0^6\\ \mathbf{H}_0^1, \mathbf{H}_0^2, \ldots, \mathbf{H}_0^6\end{pmatrix},$$

$$\mathcal{J} \equiv \begin{pmatrix}\mathbf{J}_0^1, \mathbf{J}_0^2, \ldots, \mathbf{J}_0^6\\ \mathbf{I}_0^1, \mathbf{I}_0^2, \ldots, \mathbf{I}_0^6\end{pmatrix}. \tag{5}$$

Each column of the matrices in Eq. (5) is associated with a single current-driven electromagnetic simulation that involves the solution of Eqs. (2), subject to the medium's constitutive parameters. For example, in the first simulation the driving current is $\mathcal{J}_{i1} = (1,0,0,0,0,0)$, i.e. $\mathbf{J}_0 = \mathbf{e}_x$ and $\mathbf{I}_0 = 0$; in the second simulation $\mathcal{J}_{i2} = (0,1,0,0,0,0)$, etc. Electromagnetic fields can then be combined into the matrices $\mathcal{E}$ and $\mathcal{D}$ which are, by definition, related through the CPM defined by Eq. (1). Finally, the CPM is recovered:

$$\mathsf{C} \equiv \begin{pmatrix}\varepsilon & \xi\\ \zeta & \mu\end{pmatrix} = \mathcal{D}\mathcal{E}^{-1}. \tag{6}$$

Since the six electromagnetic simulations are performed for a particular ω and $\mathbf{k}$, the calculated CPM is a function of ω and $\mathbf{k}$: $\mathsf{C} = \mathsf{C}(\omega, \mathbf{k})$. For the homogeneous medium, CDH procedure returns the *a priori* known CPM, so no new information about the medium is gained. The real utility of the CDH is that the same extraction procedure can be applied to an inhomogeneous (periodic) metamaterial if an field averaging procedure can be introduced. The field averaging procedure resulting in the *effective* CPM of the metamaterial is described below.

3. Field averaging and homogenization of periodic metamaterials

By definition, a periodic metamaterial is highly inhomogeneous. A unit cell of a metamaterial may consist of various arbitrarily shaped material inclusions such as metals and/or dielectrics. Microscopic EM fields **e**, **h**, **d** and **b** inside each of these inclusions are related through Eqs. (2), subject to the material's local constitutive parameters. In practice, solving Maxwell's equations (2) for **e**, **h**, **d** and **b** inside a single unit cell for a fixed frequency ω can be accomplished using any commercial finite elements software package, e.g., COMSOL Multiphysics. Microscopic EM fields are subject to phase-shifted periodic boundary conditions determined by the wavenumber **k**. Introducing the *effective* CPM of such metamaterial requires averaging strongly inhomogeneous microscopic fields inside the unit cell in order to obtain a matrix of *macroscopic* fields given by Eq. (5). The CDH procedure is then applied to obtain the effective CPM according to Eqs. (5) and (6).

Field averaging procedures are not unique, and several have been utilized in the past [1,4,6] to predict wave propagation inside a metamaterial. A new field-averaging procedure is introduced below. Like the earlier procedures [1,4,6], it predicts the correct dispersion relation for the propagating waves. In addition, it provides approximately correct boundary conditions [10]. The general three-dimensional volume-averaging procedure is described below, although only two-dimensional examples are provided in the rest of the paper.

Because of the unique way different components of the EM field enter the Maxwell's equations, the volume-averaging technique also treats these components differently. Specifically, the following averaging formulas are used for the field components of $(\mathbf{D}_0, \mathbf{B}_0)$ parallel to $\mathbf{k}^*$ (the * indicates complex conjugation) and the field components of $(\mathbf{E}_0, \mathbf{H}_0)$ perpendicular to $\mathbf{k}$:

$$-i\mathbf{k}\cdot\begin{Bmatrix}\mathbf{D}_0\\ \mathbf{B}_0\end{Bmatrix} S_V = \int_\Omega \frac{d^3x}{V}\nabla\cdot\begin{Bmatrix}\mathbf{d}_0\\ \mathbf{b}_0\end{Bmatrix} \tag{7}$$

and

$$-i\mathbf{k}\times\begin{Bmatrix}\mathbf{E}_0\\ \mathbf{H}_0\end{Bmatrix} S_V = \int_\Omega \frac{d^3x}{V}\nabla\times\begin{Bmatrix}\mathbf{e}_0\\ \mathbf{h}_0\end{Bmatrix}, \tag{8}$$

where integration is over the unit cell (Ω), $V = a_x a_y a_z$ is the volume of a unit cell with dimensions $a_x \times a_y \times a_z$, and S_V the is the three-dimensional generalization of the earlier introduced [11] form-factor:

$$S_V = \frac{\sin(k_x a_x/2)}{a_x k_x/2}\cdot\frac{\sin(k_y a_y/2)}{a_y k_y/2}\cdot\frac{\sin(k_z a_z/2)}{a_z k_z/2}. \tag{9}$$

For the remaining field components, a straightforward volume averaging is used:

$$\mathbf{k}^* \times \begin{Bmatrix} \mathbf{D}_0 \\ \mathbf{B}_0 \end{Bmatrix} S_V = \int_\Omega \frac{d^3x}{V} \mathbf{k}^* \times \begin{Bmatrix} \mathbf{d} \\ \mathbf{b} \end{Bmatrix} \tag{10}$$

and

$$\mathbf{k}^* \cdot \begin{Bmatrix} \mathbf{E}_0 \\ \mathbf{H}_0 \end{Bmatrix} S_V = \int_\Omega \frac{d^3x}{V} \mathbf{k}^* \cdot \begin{Bmatrix} \mathbf{e} \\ \mathbf{h} \end{Bmatrix}. \tag{11}$$

The macroscopic field components $\mathbf{E}_0$, $\mathbf{H}_0$, $\mathbf{D}_0$ and $\mathbf{B}_0$ are defined as the method of least squares solution the system of equations (7)–(11).

Different averaging recipes for different field components was also utilized in an earlier averaging scheme [1,4]. For example, without introducing different averaging recipes for $\mathbf{H}$ and $\mathbf{B}$, it would not be possible to predict effective magnetic activity ($\zeta \neq 0$ or $\mu \neq 1$) for metamaterials which do not contain any magnetic inclusions. Also, it should be noted that if $\mathbf{k}$ is parallel to the principle axis of a crystal and if the inclusions in the metamaterial are small then our averaging method for the transverse components of $\mathbf{E}_0$ and $\mathbf{H}_0$ are equivalent to the transversely averaged fields used in Ref. [12]. Finally, because of the nature of the definitions in Eqs. (7)–(11), we cannot rigorously compute the constitutive parameters at the Γ point ($\mathbf{k}=0$). It is, however, possible to compute the entire CPM for any finite wavenumber. As we show below in Section 4, finite wavenumbers introduce a new feature of metamaterials: finite bi-anisotropy caused by the spatial dispersion.

4. Bianisotropy due to spatial dispersion

It has long been recognized [2] that many recently introduced metamaterials lacking spatial inversion symmetry are bianisotropic, i.e. exhibit cross polarization effects: an electric polarization as a response to an applied magnetic field and vice versa. It is widely believed that a centro-symmetric crystal cannot be bianisotropic (ξ and ζ must be zero). However, this is only true if the constitutive parameters are functions of the frequency ω only. If the constitutive parameters are functions of both ω and $\mathbf{k}$, then spatial dispersion can cause bianisotropy even in a centrosymmetric crystal as shown below.

Consider the symmetry properties of the ζ pseudotensor under coordinate transformations characterized by the transformation matrix T (limiting ourselves to transformations where $\det(T) = \pm 1$). The pseudotensor ζ, when dependent only on ω, transforms like $\zeta'(\omega) = \det(T) T \zeta(\omega) T^{\mathrm{T}}$. For a centrosymmetric crystal, the constitutive tensors (pseudotensors) should be unchanged by the inversion $T_{\mathrm{inv}} = \mathrm{diag}(-1,-1,-1)$, implying that $\zeta(\omega) = \zeta'(\omega) = -T_{\mathrm{inv}} \zeta(\omega) T_{\mathrm{inv}}^{\mathrm{T}} = -\zeta(\omega) = 0$. However, if ζ (or ξ) is a function of $\mathbf{k}$ as well as ω, then $\zeta(\omega,\mathbf{k}) = \zeta'(\omega, T_{\mathrm{inv}}^{\mathrm{T}}\mathbf{k}) = -T_{\mathrm{inv}} \zeta(\omega, T_{\mathrm{inv}}^{\mathrm{T}}\mathbf{k}) T_{\mathrm{inv}}^{\mathrm{T}} = -\zeta(\omega,-\mathbf{k})$. Instead of showing that ζ (and ξ) vanish for a centrosymmetric crystal we obtain an important symmetry relation $\zeta(\omega,\mathbf{k}) = -\zeta(\omega,-\mathbf{k})$. There are similar symmetry relations for the other constitutive matrices for a centrosymmetric crystal: $\varepsilon(\omega,\mathbf{k}) = \varepsilon(\omega,-\mathbf{k})$, $\xi(\omega,\mathbf{k}) = -\xi(\omega,-\mathbf{k})$ and $\mu(\omega,\mathbf{k}) = \mu(\omega,-\mathbf{k})$.

Formally, the $\mathbf{k}$ vector breaks the symmetry of the crystal. This can be seen more clearly if we investigate how the pseudotensors ζ and ξ are restricted under spatial reflections. Consider the case when $\mathbf{k} = k_x\hat{\mathbf{x}}$. If we perform a reflection across the x–z plane our transformation matrix is $T_y = \mathrm{diag}(1,-1,1)$. Under this transformation, for the zy component of ζ we find $\zeta_{zy}(\omega,\mathbf{k}) = \zeta'_{zy}(\omega, T_y^{\mathrm{T}}\mathbf{k}) = \zeta_{zy}(\omega,\mathbf{k})$ since $T_y^{\mathrm{T}}\mathbf{k} = \mathbf{k}$ for $\mathbf{k} = k_x\hat{\mathbf{x}}$. Therefore, ζ_{zy} can be non-vanishing. Now consider ζ_{zx} which transforms like $\zeta_{zx}(\omega,\mathbf{k}) = \zeta'_{zx}(\omega, T_y^{\mathrm{T}}\mathbf{k}) = -\zeta_{zx}(\omega,\mathbf{k}) = 0$ for a centrosymmetric crystal. So constitutive parameters that are functions of $\mathbf{k}$ as well as ω are restricted by symmetry in different ways than constitutive parameters that are only functions of ω. Naturally, in the limit of $\mathbf{k}=0$, the $\mathbf{k}$ vector no longer breaks the symmetry of the centrosymmetric crystal, and ζ and ξ as well as the off diagonal terms in ε and μ vanish.

5. Constitutive parameters of a plasmonic metamaterial

In this section we present the results of applying the CDH approach to extract the effective CPM of a two-dimensional plasmonic metamaterial crystal known as a strip pair-one film or a SPOF [13,14]. A diagram of the SPOF is given in Fig. 1(a); it is comprised a square crystal lattice with a thin Au film in the center of the unit cell and two Au strips on both sides of the film. The permittivity of the Au is $\varepsilon = 1 - \omega_p^2/(\omega(\omega - i\Gamma))$ with $\omega_p = 1.32 \times 10^{16}$/s and $\Gamma = 1.2 \times 10^{14}$/s. The rest of the SPOF is dielectric with permittivity $\varepsilon = 1.56^2$. The SPOF structure has been shown [13] to exhibit the negative index propagation. The dispersion curves $k_x(\omega)$ corresponding to the wave propagation in the x-direction

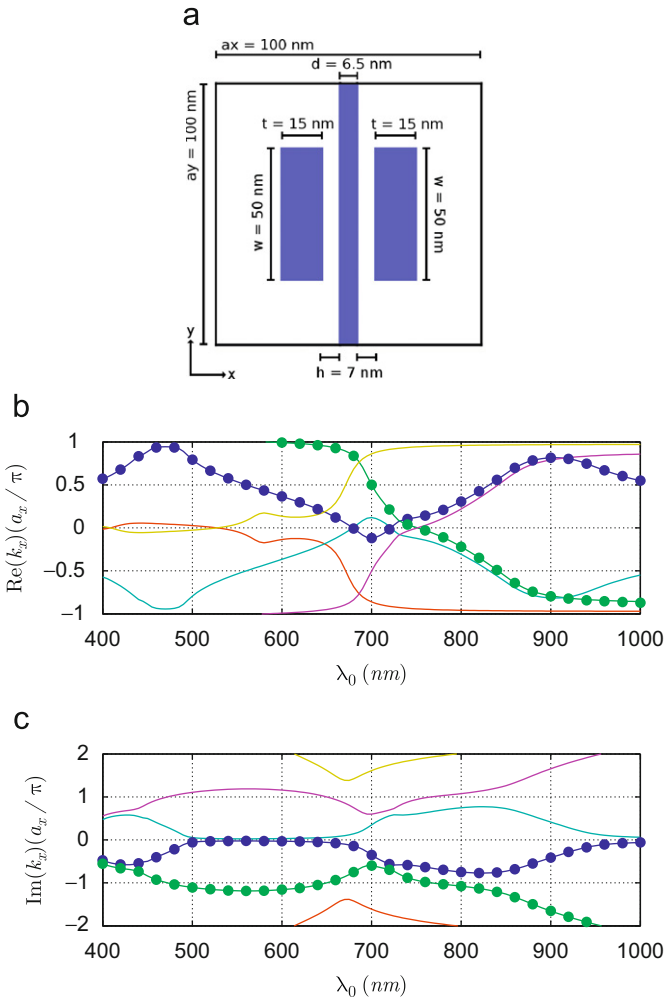

Fig. 1. Propagation of p-polarized ($\mathbf{H} = H_z(x,y)\hat{\mathbf{z}}$) waves through the two-dimensional lattice of SPOF structures. Top: the unit cell (a) of the SPOF (description in the text). Bottom: real (b) and imaginary (c) parts of k_x vs. λ_0 where $\mathbf{k} = k_x\hat{\mathbf{x}}$. Solid lines: dispersion curves $k_x(\omega)$ for a p-polarized wave obtained from an eigenvalue simulation [15]. Dotted lines: dispersion curves calculated from Eq. (12) using current driven constitutive parameters calculated from Eqs. (5) and (6) by driving the SPOF at ω and $\mathbf{k} = k_x(\omega)\hat{\mathbf{x}}$.

are obtained using the earlier described approach [15] and plotted in Figs. 1(b,c) as the solid lines. Only p-polarized modes ($\mathbf{H}=H_z(x,y)\hat{\mathbf{z}}$) are studied in the rest of the paper. Only one mode (blue line) is ever radiating, and only for certain frequency bands. All other modes are evanescent.

As the first test of the CDH approach, we have extracted the full set of current-driven constitutive parameters as functions of $(\omega,\mathbf{k}=k_x(\omega)\hat{x})$ for the eigenmodes of the crystal following the averaging and homogenization techniques described in Sections 2 and 3. The unit cell is driven slightly off the dispersion curve so as to prevent the matrix $\mathcal{M}$ in Eqs. (3) and (4) from being singular. Thus obtained entries of the CPM are used to calculate the real and imaginary parts of the complex wavenumber for each eigenmode according to the dispersion relation of the SPOF (dotted lines), which for a p-polarized wave propagating in the x-direction is given by

$$\left(\frac{k_x-\omega\zeta_{zy}/c}{\mu_{zz}}\right)\left(\frac{k_x+\omega\xi_{yz}/c}{\varepsilon_{yy}}\right)-\frac{\omega^2}{c^2}=0. \tag{12}$$

Note from Eq. (12) that only four entries of the CPM (ε_{yy}, ζ_{zy}, μ_{zz} and ξ_{yz}) affect the mode's propagation in the x-direction. Fig. 1 indicates that the current driven constitutive parameters accurately predict the correct dispersion for two of the modes, one of which (blue line) is radiative for some frequencies and evanescent for others while the other one (green line) is always evanescent. Though not shown in Fig. 1, the current-driven constitutive parameters fail to predict the dispersion of the third mode (red line) due to the mode having an antisymmetric field profile.

The constitutive parameters ε_{yy} and ζ_{zy} for the SPOF extracted along the dispersion curve $k_x(\omega)$ of the "radiative" (blue line) eigenmode are shown in Figs. 2(a,b), respectively. The CDH procedure also yields $\xi_{yz}=0$ and $\mu_{zz}=1$ for all frequencies. We conjecture that this simplification is due to two factors: that all inclusions of the SPOF possess only a local electric response, and that the SPOF is centrosymmetric structure.

Extracted $\mu_{zz}=1$ is in apparent disagreement with the results of the S-parameter retrieval [3] of $\mu_{zz}\neq 1$ for the SPOF [13] or similar negative index structures. In fact, it directly follows from Eqs. (4) and (12) that the only relevant quantity for this specific propagation direction and wave polarization is $(k_x-\omega\zeta_{zy}/c)/\mu_{zz}$. Therefore, any set of effective parameters $(\zeta_{zy}^{eff},\mu_{zz}^{eff})$ satisfying $(k_x-\omega\zeta_{zy}^{eff}/c)/\mu_{zz}^{eff}=(k_x-\omega\zeta_{zy}/c)/\mu_{zz}$, including $\zeta_{zy}^{eff}=0$ (assumed in S-parameter retrieval) and $\mu_{zz}^{eff}=(1-\omega\zeta_{zy}/ck_x)^{-1}$ are valid constitutive parameters. Thus defined μ_{zz}^{eff} is indeed extracted using S-parameter retrieval [10].

An important new capability of the CDH approach is that it can calculate the constitutive parameters of a metamaterial for any ω and $\mathbf{k}$ that do not obey the dispersion relation inside the metamaterial crystal. This has important implications for various applications, such as metamaterial-embedded antennas and quantum dots. Because an antenna can have an arbitrary shape and position, detailed knowledge of the CPM on and off the dispersion curve is necessary. Below we demonstrate a close agreement between radiation patterns of a monochromatic flat (infinitely extended in the y–z plane) directional antenna embedded inside (i) a SPOF array comprised five layers stacked in the x-direction, and (ii) a finite homogeneous 500 nm thick slab with the CPM corresponding to the SPOF metamaterial. Owing to the linear response of the metamaterial, it is sufficient to investigate radiation patterns (transmission from the left and right slab boundaries) for the electric currents in the form of $\mathbf{J}_\mathbf{k}=J_0\hat{\mathbf{y}}e^{i(\omega t-\mathbf{k}\cdot\mathbf{x})}$. For example, a flat antenna with a finite size in

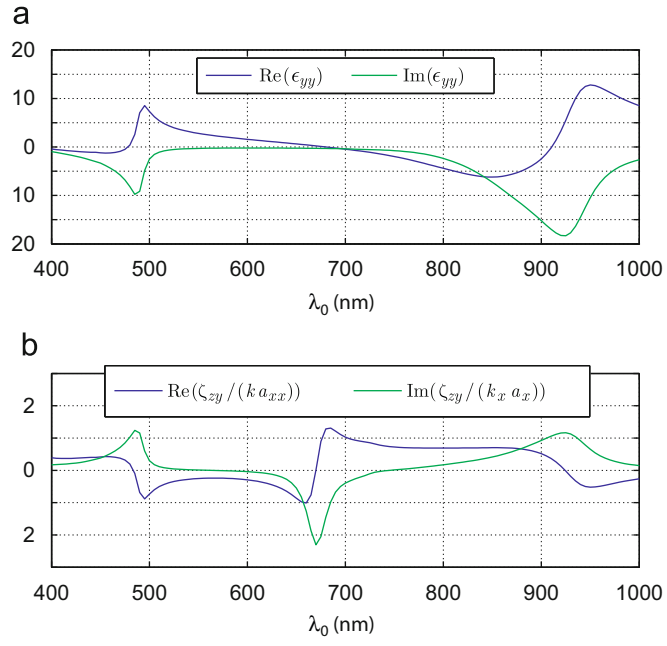

Fig. 2. Constitutive parameters of the two-dimensional lattice of SPOF structures (see Fig. 1): ε_{yy} (a) and $\zeta_{zy}/(k_x a_x)$ (b) computed using Eqs. (5) and (6) along the "radiative" dispersion curve $\mathbf{k}=k_x(\omega)\hat{\mathbf{x}}$ shown in Fig. 1 as a blue line. Not shown: $\mu=1$, $\xi=0$ for all wavelengths. (For interpretation of the references to color in this figure legend, the reader is referred to the web version of this article.)

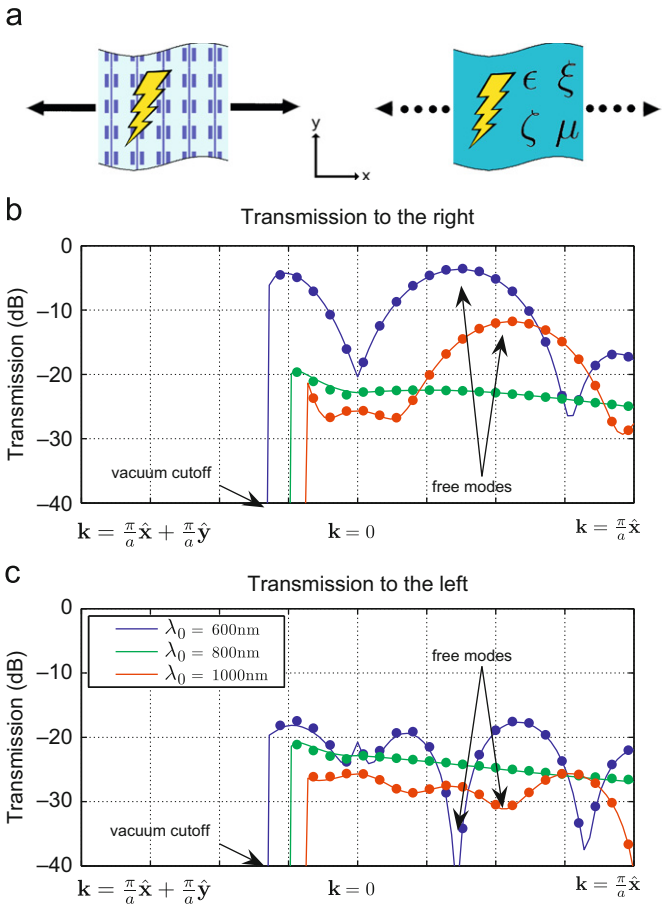

Fig. 3. Radiation by the harmonic current $\mathbf{J}_\mathbf{k}=J_0\hat{\mathbf{y}}e^{i(\omega t-\mathbf{k}\cdot\mathbf{x})}$ emulating a directional antenna embedded inside a metamaterial slab. Radiation emerging from the right (a) and left (b) boundaries of the slab is plotted for the current embedded inside a five-layer thick SPOF metamaterial (solid lines) and a $L=500$ nm homogeneous slab with the CPM of the SPOF (dotted lines).

the x-direction can be represented as a superposition of such currents summed over a spectrum of $\mathbf{k}$.

The results of the simulations for the cases (i) and (ii) carried out for a wide spectrum of $\mathbf{k}$'s are shown in Fig. 3 as solid lines and dots, respectively. All simulations were performed for three antenna frequencies corresponding to $\lambda_0 = 600$, 800, and 1000 nm. The wavenumbers $\mathbf{k}$ are varied from $\mathbf{k} = 0$ to $\mathbf{k} = \pi/a\hat{\mathbf{x}}$ (right half of Fig. 3) and from $\mathbf{k} = 0$ to $\mathbf{k} = \pi/a\hat{\mathbf{x}} + \pi/a\hat{\mathbf{y}}$ (left half of Fig. 3). Finite value of k_y enables steering the beam at an angle with respect to the slab's boundary. For the homogeneous medium we assumed Maxwell boundary conditions (continuity of tangential $\mathbf{E}$ and $\mathbf{H}$ fields). The radiation flux escaping through the right and left slab's boundaries are shown in Figs. 3(a) and (b), respectively.

Strong antenna directionality is observed for $\lambda_0 = 600$ and 1000 nm antennas which can couple to the low-loss propagating modes: the peaks of the forward flux are matched by the dips of the backward flux. Such phase matching is achieved when $\mathbf{k}$ matches $\mathrm{Re}(\mathbf{k}(\omega))$ on the dispersion curve in Fig. 1(b). Directionality of the $\lambda_0 = 800$ nm antenna is poor because at this frequency all free modes in the SPOF are evanescent according to Fig. 1(c). Very good agreement between the simulations of the cases (i) and (ii) is observed, confirming the accuracy of the homogenization procedure. The small observed discrepancies are believed to be mostly due to the imperfect boundary conditions.

6. Conclusion

In conclusion, a new homogenization technique for metamaterial crystal is introduced. The combination of the current-driven homogenization technique and a new averaging procedure for the microscopic EM fields of the crystal yields the full constitutive parameters matrix of a metamaterial as a function of the frequency and propagation wavenumber. A new result obtained using this technique is the demonstration of bianisotropy of a centrosymmetric crystal due to spatial dispersion. The theory appears highly accurate at predicting the dispersion of free waves in a metamaterial crystal. Our method can also calculates constitutive parameters away from the dispersion curve which is necessary for computing Green's function solutions for the currents embedded inside a metamaterial.

Acknowledgments

This work was supported by the AFOSR MURI under Grants no. FA9550-06-1-0279 and no. FA9550-08-1-0394, and the NSF NIRT under Grant no. 0709323.

References

[1] J.B. Pendry, A.J. Holden, D.J. Robbins, W.J. Stewart, IEEE Trans. Microwave Theory Technol. 47 (1999) 2075.
[2] R. Marques, F. Medina, R. Rafii-El-Idrissi, Phys. Rev. B 65 (2002) 144440.
[3] D.R. Smith, S. Schultz, P. Markos, C.M. Soukoulis, Phys. Rev. B 65 (2002) 195104.
[4] D.R. Smith, J.B. Pendry, J. Opt. Soc. Amer. B 23 (2006) 391.
[5] R. Lui, T.J. Cui, D. Huang, B. Zhao, D.R. Smith, Phys. Rev. E 76 (2007) 026606.
[6] M.G. Silveirinha, Phys. Rev. B 75 (2007) 115104.
[7] J.A. Kong, Electromagnetic Wave Theory, Wiley, New York, 1986.
[8] J.D. Jackson, Classical Electrodynamics, third ed., Wiley, Hoboken, 1998, pp. 273–274.
[9] F. Moulin, Il Nuovo Cimento B 116B (2001) 869.
[10] C. Fietz, G. Shvets, Metamaterial homogenization: extraction of effective constitutive parameters, in: M.A. Noginov, N.I. Zheludev, A.D. Boardman, N. Engheta (Eds.), Metamaterials, SPIE, Bellingham, WA, 2009, p. 739219.
[11] D.R. Smith, D.C. Vier, N. Kroll, S. Schultz, Appl. Phys. Lett. 77 (2000) 2246.
[12] C.R. Simovski, Metamaterials 1 (2007) 62.
[13] V. Lomakin, Y. Fainman, Y. Urzhumov, G. Shvets, Opt. Exp. 14 (2006) 11164.
[14] Y.A. Urzhumov, G. Shvets, Solid State Commun. 146 (2008) 208.
[15] M. Davanco, Y. Urzhumov, G. Shvets, Opt. Exp. 15 (2007) 9681.